

Protein-Grafted Polymers Prepared Through a Site-Specific Conjugation by Microbial Transglutaminase for an Immunosorbent Assay

Rie Wakabayashi,^{*,†,‡,§} Kensuke Yahiro,[†] Kounosuke Hayashi,^{†,‡,§} Masahiro Goto,^{†,§} and Noriho Kamiya^{*,†,§}

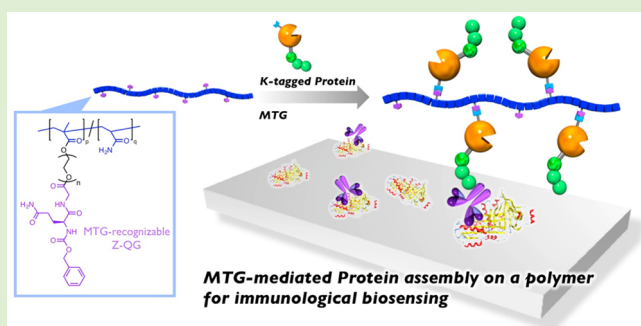
[†]Department of Applied Chemistry, Graduate School of Engineering, Kyushu University, 744 Motooka, Nishi-ku, Fukuoka 819-0395, Japan

[‡]Hitachi Aloka Medical, Ltd., 3-7-19 Imai, Ome-shi, Tokyo 198-8577, Japan

[§]Division of Biotechnology, Center for Future Chemistry, Kyushu University, 744 Motooka, Nishi-ku, Fukuoka 819-0395 Japan

S Supporting Information

ABSTRACT: Protein–polymer conjugates have been developed in many fields. Most hybrids are composed of one protein attached to one or several polymer chains. The other form of hybrid involves the construction of multiple proteins on one polymer chain, thereby facilitating protein assemblies that provide multivalent effects. Unfortunately, synthetic methods for production of these types of hybrids are limited and challenging because precise control of the conjugation sites is needed. Herein, a novel synthetic polymer that can enzymatically assemble multiple proteins was developed. Polyacrylamide grafted with multiple microbial transglutaminase (MTG)-recognizable peptide derivatives was synthesized, and MTG-catalyzed site-specific conjugation of proteins with the polymer was achieved. The application for immunological biosensing was demonstrated using the assembly of a fusion protein composed of antibody-binding and enzyme moieties. This enzymatic method to synthesize a one-dimensional protein assembly on a synthetic polymer is versatile and can be expanded to a wide range of applications.



INTRODUCTION

Conjugation of naturally occurring functional macromolecules, for example, proteins, with artificial materials has been developed to realize a novel and unique property of the conjugates or to expand the use of the intrinsic protein functions. The molecules or materials to be conjugated with proteins include small molecules, synthetic polymers, nanoparticles, and surfaces. Among the hybrids with these molecules/materials, protein–polymer hybrids have been vigorously studied in many research and industrial fields.^{1–6} Synthetic polymers can be designed with diverse chemical structures; therefore, proteins can acquire modulated physical properties, chemical stability, and sometimes stimuli responsiveness derived from polymer properties.⁷ One of the most successful applications of protein–polymer hybrids is PEGylation; the covalent conjugation of a protein with poly(ethylene glycol) (PEG).^{8–11} The enhanced pharmacokinetic properties of PEGylated proteins, such as longer half-lives in blood, lower immunogenicity, and increased stability against enzymatic degradation, have enabled lower doses and less frequent administration of biopharmaceuticals.

The majority of the protein–polymer conjugates reported thus far are composed of one protein attached to one or several

polymer chains. These conjugates are fabricated mainly to modulate protein properties. Another form of hybrids is multiple proteins mounted onto a polymer chain, thus facilitating the assembly of multiple proteins in one structure.^{12,13} Besides the benefits described above, these structures provide the important feature of multivalency. Multivalent protein clusters are expected to show better cascade reactions,^{12–17} cooperative enzymatic reactions,^{18,19} stable immobilization of enzymes on solid supports,^{20–22} and higher affinity toward targeted molecules for biosensing.^{23–30}

A common method to prepare protein–polymer hybrids is to use natural reactive amino acids, such as lysines and cysteines, for the chemical modification of polymers bearing reactive groups. Unfortunately, proteins often contain a number of these reactive amino acids and thus a chemical reaction can occur randomly, which leads to random conjugation numbers and sometimes to an undesired loss of protein function. Indistinct conjugation sites are especially problematic in an attempt to fabricate multiple proteins–polymer hybrids

Received: October 18, 2016

Revised: December 13, 2016

Published: December 14, 2016

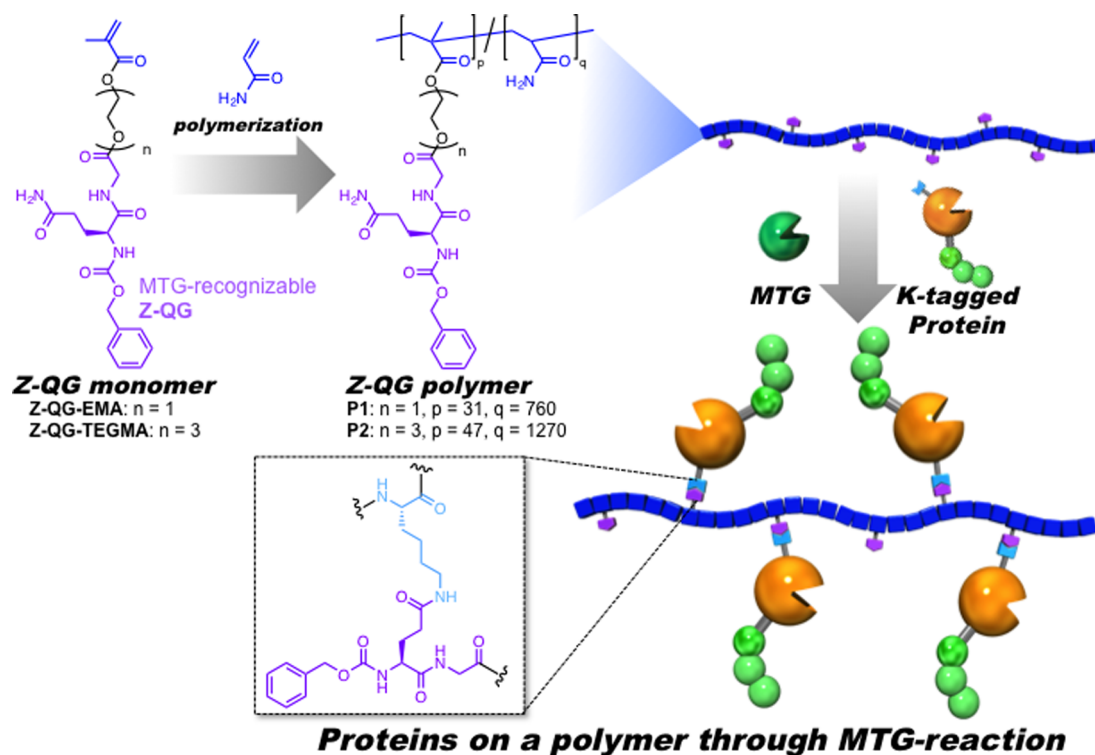


Figure 1. Schematic representation of this study. The microbial transglutaminase (MTG)-recognizable *N*-benzyloxycarbonyl-L-glutaminyglycine (Z-QG)-containing monomer was polymerized using acrylamide as a comonomer and the resultant Z-QG polymer worked as a scaffold to assemble lysine (K)-tagged proteins by MTG catalysis.

because random conjugation may lead to a cross-linking of proteins that results in gelation.³¹ To solve these problems, site-specific modification methods have been developed, which include utilization of an N-terminal amino group that has different protonation properties than lysine residues, protein engineering to introduce unnatural amino acids, and enzymatic reactions. An enzymatic strategy is attractive because enzymes intrinsically possess substrate specificity.³² The preparation of 1:1 protein/polymer conjugates has been achieved using enzymes such as transglutaminase,^{33–36} sortase,^{37,38} *N*-acetylgalactosaminyltransferase,³⁹ farnesyltransferase,⁴⁰ and formylglycine-generating enzyme.⁴¹

We have developed previously a microbial transglutaminase (MTG)-mediated conjugation of multiple proteins on nucleic acids.^{18,26} MTG functions as a biocatalysis for the acyl-transfer reaction between the γ -carboxamide of glutamine (Q) residues and the ϵ -amino group of lysine (K) residues or primary amines.^{42,43} MTG-recognizable peptides can be introduced at both the N- and C-termini of proteins and within internal loop sequences.⁴⁴ A short peptide derivative, *N*-benzyloxycarbonyl-L-glutaminyglycine (Z-QG), is known as an MTG-reactive glutamine substrate, which enabled us to synthesize an MTG-reactive DNA/RNA scaffold by the polymerase chain reaction. The scaffolds were functionalized with different types of enzymes and the resultant enzyme assemblies showed potential use in diagnostic applications.^{18,19} These examples clearly revealed the applicability of the MTG reaction to realize protein assemblies on a one-dimensional polymeric scaffold.

In this study, we developed a synthetic polymer scaffold that can assemble multiple proteins site-specifically through the MTG reaction. Several research groups have reported the site-specific conjugation of synthetic polymers to proteins using MTG; in these reports, however, intrinsic MTG-recognizable

glutamine residues in native proteins that were discovered experimentally were reacted with polymers bearing amino groups at the end position.^{33–36} In contrast, our approach is introducing multiple MTG-reactive Z-QG groups into synthetic polymers and MTG-recognizable K-tags (MRHKGS) to proteins. Because Z-QG is a synthetic short peptide derivative, the synthetic route for Z-QG bearing polymers is readily accessible. A novel polymer containing Z-QG moieties was prepared and genetically engineered proteins bearing MTG-recognizable K-tags (MRHKGS) were conjugated with the polymer without a noticeable loss of protein functions (Figure 1). A possible application for immunological biosensing was demonstrated by the assembly of an artificial fusion protein composed of antibody-binding and alkaline phosphatase moieties. To our knowledge, this is the first report of enzymatically prepared protein assemblies on a synthetic polymer.

EXPERIMENTAL SECTION

Materials. MTG was kindly provided by Ajinomoto Co., Inc. (Tokyo, Japan). Wild-type enhanced green fluorescent protein (wt-EGFP) and recombinant EGFP fused with a C-terminal MTG-recognizable K-tag (Ktag-EGFP) were prepared by the previously reported procedure.⁴⁵ The concentrations of these proteins were determined using the molar extinction coefficient of $55\,000\text{ M}^{-1}\text{ cm}^{-1}$ at 488 nm. A K-tagged fusion protein composed of a chimera alkaline phosphatase (IPP) and antibody Fc-binding domain (PG), Ktag-IPP-PG, was produced using a mammalian cell line FreeStyle 293F by a previously reported protocol.⁴⁶ Briefly, the constructed pcDNA_IPP-PG vector was transfected to FreeStyle 293F cells using Lipofectamine LTX PLUS (Thermo Fisher Scientific, Waltham, MA, U.S.A.). The cells were incubated at 37 °C for 72 h under 5% CO₂ atmosphere and the culture media containing secreted proteins were filtered through a 0.22- μm membrane filter. N- and C-terminal sequences for the above

proteins are listed in Table S1. All chemicals for the preparation of Z-QG polymers were used as received without further purification. Z-QG, 2-hydroxyethyl methacrylate (HEMA), and polyethylene glycol/poly(ethylene oxide) analytical standard, ReadyCal set (M_p 200–1 200 000) were purchased from Sigma-Aldrich (St Louis, MO, U.S.A.). Triethylene glycol (TEG) and methacryloyl chloride were purchased from Tokyo Kasei (Tokyo, Japan). N,N' -dicyclohexylcarbodiimide (DCC), 1-benzotriazol monohydrate (HOBt), and N,N -dimethylaminopyridine (DMAP) were purchased from Watanabe Chemical Industries, Ltd. (Hiroshima, Japan). N,N -Dimethylformamide (DMF), 2,2'-azobis(isobutyronitrile) (AIBN), acrylamide, and LiBr were purchased from Wako Pure Chemicals Industries, Ltd. (Osaka, Japan). Dimethyl sulfoxide (DMSO) was purchased from Kishida Chemical Co., Ltd. (Osaka, Japan).

General. ^1H NMR spectra were recorded on a 300-MHz Bruker AV300M. CDCl_3 or $(\text{CD}_3)_2\text{SO}$ (Wako) was used as the solvent. Chemical shifts are reported as δ/ppm relative to tetramethylsilane (δ/ppm 0) or residual internal $(\text{CD}_3)_2\text{SO}$ (δ/ppm 2.5). Gel permeation chromatography (GPC) was performed on a LaChrom Elite system (Hitachi High-Technologies Co., Tokyo, Japan) equipped with a GL-7410 pump and a GL-7454 differential refractive index (RI) detector using a Shodex OHPak SB-8066 M HQ column. The mobile phase used was DMSO/water = 40:60, containing 5 mM LiBr and the flow rate was 0.3 mL/min. Polyethylene glycol (M_p 200–1 200 000) was used as the standard. MALDI-TOF-MS was measured with a Bruker Autoflex-III using α -cyano-4-hydroxycinnamic acid (CHCA) as the matrix.

Synthesis of Z-QG Monomers. 2-(N -Benzyloxycarbonyl-L-glutaminyglycyloxy)-ethyl Methacrylate (Z-QG-EMA). To a DMF solution (15 mL) of Z-QG (0.51 g, 1.5 mmol), HEMA (0.39 g, 3.0 mmol), DCC (0.37 g, 1.8 mmol), and HOBt (0.29 g, 1.9 mmol) DMAP (37 mg, 0.30 mmol) was added at 0 °C. The temperature was allowed to rise gradually to room temperature, then to 40 °C. The reaction mixture was further stirred at 40 °C for 20 h. The white precipitate was removed by filtration and the solvent was evaporated under reduced pressure. A small amount of DMSO was added to the waxy residue and this residue was diluted with ethyl acetate. The organic layer was washed with aqueous solutions of 10% citric acid, 5% sodium bicarbonate, brine, and dried over anhydrous sodium sulfate. The solvent was removed under reduced pressure to give Z-QG-EMA as a white powder (0.63 g, 93%). ^1H NMR (300 MHz, $(\text{CD}_3)_2\text{SO}$, δ/ppm): 1.70–1.74 (m, 2H), 1.88 (s, 3H), 2.13 (t, $J = 7.2$ Hz, 2H), 3.83–3.89 (m, 2H), 3.97–4.04 (m, 1H), 4.30 (br, 4H), 5.02 (s, 2H), 5.69 (s, 1H), 6.04 (s, 1H), 6.76 (br, 1H), 7.24 (br, 1H), 7.36 (br, 5H), 7.47 (d, $J = 7.8$ Hz, 1H), 8.33 (t, $J = 5.7$ Hz, 1H). ^{13}C NMR (75 MHz, $(\text{CD}_3)_2\text{SO}$), δ/ppm): 18.0, 27.7, 31.4, 40.6, 54.2, 62.3, 62.4, 65.4, 126.2, 127.7, 127.8, 128.3, 135.5, 137.0, 155.9, 156.6, 166.4, 169.7, 172.3, 173.7. Full ^1H and ^{13}C NMR spectra can be found in Supplementary Figures S1 and S2, respectively.

2-(2-(2-Hydroxyethoxy)ethoxy)ethyl Methacrylate (TEGMA). Triethylene glycol (3.4 mL, 25.7 mmol) was dissolved in a mixture of dichloromethane (80 mL) and pyridine (2.1 mL) and the solution was purged with argon for 30 min at room temperature. The solution was cooled to 0 °C and a dichloromethane solution (10 mL) of methacryloyl chloride (2.4 mL, 24.8 mmol) was added dropwise. The solution was stirred at 0 °C for 2 h and then at room temperature for 2 h. The solvent was removed under reduced pressure and the crude material was purified by column chromatography (silica gel, ethyl acetate/*n*-hexane = 7/3) to give TEGMA as a colorless oil (2.17 g, 40%). ^1H NMR (300 MHz, CDCl_3 , δ/ppm): 1.96 (s, 3H), 3.60–3.78 (m, 10H), 4.31–4.34 (m, 2H), 5.59 (s, 1H), 6.15 (t, $J = 0.75$ Hz, 1H).

2-(2-(2-(N -Benzyloxycarbonyl-L-glutaminyglycyloxy)ethoxy)ethoxy)ethyl Methacrylate (Z-QG-TEGMA). Z-QG-OH (0.50 g, 1.5 mmol) and TEGMA (0.44 g, 1.7 mmol) were dissolved in DMF (15 mL). The solution was cooled to 0 °C and purged with argon. DCC (0.37 g, 1.8 mmol), HOBt (0.28 g, 1.8 mmol), and DMAP (37.0 mg, 0.3 mmol) were added at 0 °C and the temperature was allowed to rise gradually to room temperature. The solution was further stirred at 40 °C for 23 h under argon atmosphere. The white precipitate was

filtered off and the solvent was removed under reduced pressure. Ethyl acetate was added to the residue and the organic phase was washed with 5% sodium bicarbonate and brine then dried over anhydrous sodium sulfate and evaporated. The resultant solid material was purified by column chromatography (silica gel, dichloromethane/methanol = 15/1) to give Z-QG-TEGMA as a white powder (0.55 g, 69%). ^1H NMR (300 MHz, $(\text{CD}_3)_2\text{SO}$ δ/ppm): 1.72 (m, 2H), 1.88 (s, 3H), 2.14 (m, 2H), 3.54 (br, 4H), 3.60 (br, 4H), 3.82–3.88 (m, 2H), 4.02 (m, 2H), 4.15 (br, 2H), 4.21 (m, 2H), 5.02 (s, 2H), 5.69 (s, 1H), 6.03 (s, 1H), 6.76 (br, 1H), 7.25 (br, 1H), 7.36 (br, 5H), 7.47 (d, $J = 7.5$ Hz, 1H), 8.31 (br, 1H). ^{13}C NMR (75 MHz, $(\text{CD}_3)_2\text{SO}$ δ/ppm): 18.0, 27.7, 31.4, 40.6, 54.3, 63.7, 63.8, 65.5, 68.2, 69.8, 125.9, 127.7, 127.8, 128.4, 135.8, 137.0, 155.9, 166.6, 170.0, 172.2, 173.8. Full ^1H and ^{13}C NMR spectra can be found in Supplementary Figures S3 and S4, respectively.

Synthesis and Characterization of Z-QG Polymers. Z-QG Polymer P1. Z-QG polymer P1 was synthesized by radical polymerization using acrylamide as a comonomer at a 4:96 molar ratio of Z-QG-EMA:acrylamide. A mixture of Z-QG-EMA (0.040 M), acrylamide (0.96 M), and AIBN (10 mM) in DMSO (1.0 mL) was purged with argon for 15 min. The solution was stirred at 60 °C for 56 h. A small amount of water was added and the polymer was recovered from the mixture by precipitation from cold acetone. The white precipitate was collected and dried in vacuo. The resultant white solid was dissolved in water and lyophilized to give the Z-QG polymer P1 as a white powder. Analysis of ^1H NMR spectrum ($(\text{CD}_3)_2\text{SO}$) revealed that the Z-QG-EMA/acrylamide = 3.9:96.1 by comparing the integrals of peaks corresponding to benzyl protons for Z-QG-EMA (δ 5.03) and protons of the main chain of acrylamide (δ 1.53, 2.16) (Supplementary Figure S5). GPC analysis showed $M_n = 68.0$ kDa, $M_w = 305$ kDa and PDI = 4.49.

Z-QG Polymer P2. Z-QG polymer P2 was synthesized by the same procedure as P1 except that Z-QG-TEGMA was used instead of Z-QG-EMA. ^1H NMR analysis revealed the ratio Z-QG-TEGMA:acrylamide to be 3.6:96.4 (Supplementary Figure S6). The GPC chromatogram indicated $M_n = 115$ kDa, $M_w = 344$ kDa and PDI = 2.98.

MTG-Mediated Conjugation of Z-QG Monomers with Ktag-EGFP. A mixture of Ktag-EGFP (10 μM) and Z-QG-EMA or Z-QG-TEGMA (200 μM) was prepared in 10 mM Tris-HCl buffer (pH 8.0). MTG (0.5 U/mL) was added to the solution and the reaction was allowed to proceed at 25 °C for 1 h. Ten microliters were withdrawn from the reaction mixture at 5, 10, 30, and 60 min after MTG was added and 40 μL of 0.1% TFA/water was added to terminate the MTG reaction. The reaction was evaluated by MALDI-TOF-MS analysis. As a control, the reaction was performed using wt-EGFP instead of Ktag-EGFP.

Conjugation Reaction of Ktag-EGFP and Z-QG Polymers. MTG (1.0 U/mL) was added to a mixture of Ktag-EGFP (10 μM) and Z-QG polymer P1 or P2 (200 μM /Z-QG unit) in 100 mM citrate buffer (pH 5.8). The concentrations of the Z-QG units in the Z-QG polymer solutions were calculated from the weight of the polymer and the average Z-QG content determined by ^1H NMR. After the reaction at 25 °C for 3 h, N -ethylmaleimide (NEM, Kishida Chemical Co., Ltd.) was added at a final concentration of 1 mM to deactivate MTG. As negative controls, samples using wt-EGFP instead of Ktag-EGFP or in the absence of MTG were prepared. Each sample was analyzed by sodium dodecyl sulfate polyacrylamide gel electrophoresis (SDS-PAGE) (ATTO e-PAGEL E-R1020L, 20 mA, 110 min). After electrophoresis, protein bands were stained with a Quick-CBB PLUS solution (Wako). The conjugation ratio was evaluated by comparing the band intensities of EGFP with and without MTG addition using the ImageJ software.⁴⁷

The influence of the MTG reaction on protein functions of Ktag-EGFP was evaluated by fluorescence spectroscopy. The reaction mixture was diluted 100-fold using 10 mM Tris-HCl (pH 8.0). The fluorescence spectra were recorded on a PerkinElmer LS55 with an excitation wavelength of 460 nm at 25 °C. The fluorescence intensities with and without the MTG reaction were compared for each Z-QG polymer.

Influence of Buffer Conditions on MTG-Mediated Conjugation between Ktag-EGFP and Z-QG Polymer P2. MTG reaction mixtures of Ktag-EGFP (10 μM), Z-QG polymer P2 (200 μM /Z-QG unit), and MTG (0.5 or 1 U/mL) were prepared in the following buffer solutions: 10 mM phosphate buffer (pH 5.5, 6.0, 6.5, 6.9); 10 mM citrate buffer (pH 4.8, 5.3, 6.0, 6.3); 10 mM acetate buffer (pH 4.6, 5.1, 5.6); and pH 5.8 citrate buffer (10, 50, 100 mM). Each reaction was performed at 25 °C for 3 h. After each reaction, samples were applied to an SDS-PAGE gel (ATTO e-PAGEL E-R1020L, 20 mA, 110 min). The intensities of CBB-stained bands corresponding to Ktag-EGFP were analyzed to evaluate the conjugation ratio.

Conjugation Reaction between Ktag-IPP-PG and Z-QG Polymer. Ktag-IPP-PG (5 μM), Z-QG polymer P2 (200 μM /Z-QG unit), and MTG (0.5 U/mL) were mixed in the following buffers: 10 mM acetate buffer (pH 4.6, 5.1, 5.6); 10 mM citrate buffer (pH 4.8, 5.3, 5.8, 6.3); and 10 mM Tris-HCl (pH 7.1, 7.6, 8.0, 8.5). The reaction mixtures were incubated at 25 °C for 2 h. NEM at a final concentration of 1 mM was added and the reaction ratio was analyzed by SDS-PAGE, as mentioned above. To control the number of proteins per polymer chain, the MTG-mediated conjugation was also performed using different concentrations of the Z-QG polymer (75, 100 μM /Z-QG unit). The samples were prepared in 10 mM acetate buffer (pH 5.1, 5.6) or 10 mM citrate buffer (pH 5.3) and incubated at 25 °C for 3 h in the presence of MTG (0.5 U/mL).

The influence of the MTG reaction on the enzymatic activities of Ktag-IPP-PG was investigated by a colorimetric assay using *p*-nitrophenylphosphate (*p*-NPP, Kishida Chemical Co., Ltd.) as the substrate. The MTG reaction samples were diluted 500-fold with 1 M Tris-HCl (pH 8.0) to afford 10 nM Ktag-IPP-PG solutions. Equal amounts of the Ktag-IPP-PG solution and 2 mM *p*-NPP solution in 1 M Tris-HCl (pH 8.0) were mixed and the enzymatic hydrolysis reactions were monitored by measuring the absorbance at 410 nm using a microplate spectrophotometer (Biotek, PowerWaveX). The reaction proceeded at 37 °C for 30 min. The product concentrations were plotted against the reaction time and the initial velocities, determined from the slopes of the plots at the beginning of the reaction, were used to evaluate the enzyme activities. The enzymatic activities are shown as relative values using untreated Ktag-IPP-PG as the standard.

Purification of the Ktag-IPP-PG–Z-QG Polymer Conjugate by Size Exclusion Chromatography (SEC). Ktag-IPP-PG (5 μM), Z-QG polymer P2 (75 μM /Z-QG unit), and MTG (0.5 U/mL) were mixed in 10 mM acetate buffer (pH 5.6) and the reaction was conducted at 25 °C for 6 h (total volume: 500 μL). The reaction was terminated by the addition of NEM to a final concentration of 1 mM. One hundred microliters of 10 mM Tris-HCl (pH 8.0) was added to the mixture and the combined solution was applied to a BioRad BioLogic DuoFlow system using a GE Healthcare Superdex 200 10/300 GL column. The mobile phase was 10 mM Tris-HCl (pH 8.0) containing 200 mM NaCl at a flow rate of 0.5 mL/min. Ferritin (440 kDa) and Conalbumin (75 kDa) were used as molecular weight markers (GE Healthcare Bio-Sciences). Fractions containing the IPP-PG–Z-QG polymer conjugate and Ktag-IPP-PG alone were collected, which were applied to an ultrafiltration unit using a Merck Amicon Ultra centrifugal filter (NMWL: 30 K) for the concentration and desalination. The purities of the fractions were analyzed by SDS-PAGE.

Scanning Probe Microscopy (SPM) Imaging. The purified IPP-PG–Z-QG polymer or Ktag-IPP-PG solution was diluted 10- or 100-fold with 10 mM citrate buffer (pH 5.6). A 4 μL droplet of the above diluted solution was placed onto a freshly cleave mica (Nilaco Corp., Tokyo, Japan) and incubated at room temperature for 3 min. The surface of the mica was rinsed with ultrapure water and allowed to dry under ambient conditions. The SPM images were obtained with a Hitachi Nanocute in the dynamic force mode using a SI-DF3P2 (Hitachi) cantilever.

Enzyme-Linked Immunosorbent Assay (ELISA) using the IPP-PG Assembly. *Specific Detection of OVA.* Aqueous solutions of ovalbumin (OVA; Sigma-Aldrich) (10 $\mu\text{g}/\text{mL}$) were added to a Nunc maxisorp flat-bottom 96 well plate (Thermo scientific). The well plate

was incubated at 4 °C overnight and then washed with Tris buffered saline containing 0.1% Tween 20 (TBST; 0.1% Tween 20, 10 mM Tris-HCl, 150 mM NaCl, pH 7.4). To reduce nonspecific binding, 200 μL of a 2 w/v% bovine serum albumin (BSA; Wako) solution in Tris buffered saline (TBS; 10 mM Tris-HCl, 150 mM NaCl, pH 7.4) was added and the wells were incubated at 25 °C for 2 h. Rabbit anti-OVA IgG (Sigma-Aldrich) was diluted 80 000-fold using TBS containing 2 w/v% BSA and 100 μL of the solution was added to the wells, incubated at 25 °C for 2 h, then washed with TBST. One hundred microliters of the purified IPP-PG–Z-QG polymer conjugate was added to the plate and incubated at 25 °C for 2 h, then washed with TBST. Colorimetric substrate *p*-NPP (1 mM in 1 M Tris-HCl, pH 8.0) was added and incubated at 37 °C for 30 min. The reaction was then stopped by the addition of 1 M NaOH. The detection of OVA was determined by the absorption at 410 nm measured by a microplate spectrophotometer (Biotek, PowerWaveX). As a control, Ktag-IPP-PG instead of the IPP-PG–Z-QG polymer conjugate was used for the detection of OVA.

Detection Sensitivity of OVA. Various concentrations of OVA (100 μL , 0–10 000 ng/mL) were added to a Nunc maxisorp flat-bottom 96-well plate and the ELISA was executed using the same procedure as above, except that the *p*-NPP solution for detection was incubated at 37 °C for 1 h.

OVA Detection by Dot Blotting using the IPP-PG Assembly. Aqueous solutions of OVA (1 μL of 1–56 $\mu\text{g}/\text{mL}$ OVA) were dropped on a Hybond-P PVDF membrane (GE Healthcare Bio-Sciences) and the membrane was dried under ambient conditions. Nonspecific detection was reduced by soaking the membrane in 5 w/v% skim milk in TBS at 25 °C for 1 h. Rabbit anti-OVA IgG was diluted 4000-fold in TBST and the membrane was soaked in the solution at 4 °C for 14 h. The membrane was added into the purified IPP-PG–Z-QG polymer conjugate solution in TBST at 25 °C for 2 h. Detection was achieved using CDP-Star (Roche) as a chemiluminescence agent on a Bio-Rad ChemiDoc XRS Plus system.

RESULTS AND DISCUSSION

Design of MTG-Reactive Z-QG Monomers and Synthesis and Characterization of Z-QG Polymers. To produce MTG-recognizable synthetic polymers, we introduced a polymerizable methacrylate group to a general MTG substrate bearing an MTG-reactive glutamine residue, Z-QG. 1-Hydroxyethyl methacrylate was reacted with Z-QG to yield an ester Z-QG-EMA composed of Z-QG and methacrylate (Scheme S1). Another MTG-reactive monomer, Z-QG-TEGMA, has a triethylene glycol linker between the Z-QG and methacrylate moieties. Because the active site of MTG is buried about 16 Å from the protein surface,⁴⁸ we assumed that the introduced linker would increase the reaction efficiency by reducing the steric hindrance between MTG and the polymer backbone. The MTG reactivity of the Z-QG monomers, Z-QG-EMA and Z-QG-TEGMA, was confirmed by using Ktag-EGFP as a Lys-substrate. Ktag-EGFP is appended with an MTG-reactive Lys-tag, MRHKGS, at the C-terminus.⁴⁵ Ktag-EGFP and Z-QG-EMA or Z-QG-TEGMA were treated with MTG and the reaction was monitored by MALDI-TOF-MS. The peak corresponding to Ktag-EGFP [$M + H$]⁺ gradually shifted to a higher m/z and the reaction reached a plateau within 30 min (Figure 2). The found m/z values were 28 451.1 and 28 873.3 for Z-QG-EMA, and 28 444.3 and 28 951.9 for Z-QG-TEGMA before and after the MTG reaction, respectively. The differences in m/z were similar to the molecular weights of Z-QG monomers (449.46 and 537.57 for Z-QG-EMA and Z-QG-TEGMA, respectively) subtracted by that of ammonia (17.03). The conjugation with more than 2 monomers was not observed, indicating site-specific reaction at the lysine residue in the K-tag of Ktag-EGFP.

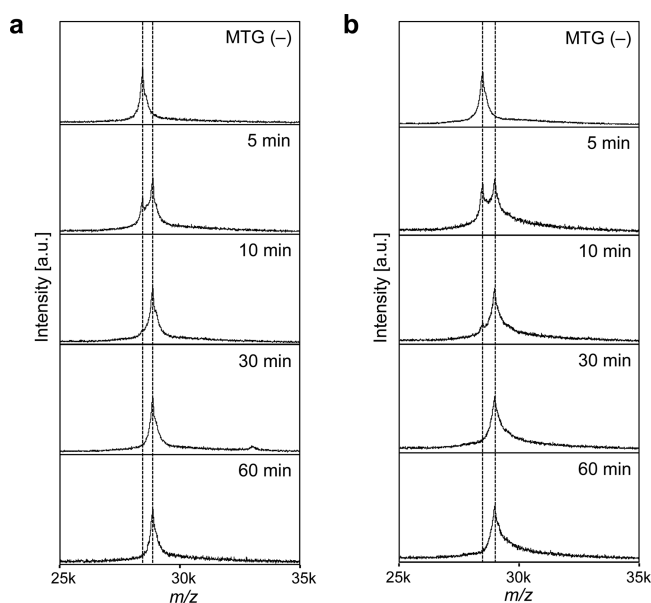


Figure 2. MALDI-TOF-MS analysis of MTG-catalyzed conjugation of EGFP fused with a C-terminal MTG-recognizable K-tag (Ktag-EGFP) with Z-QG monomers; Z-QG-EMA (a) or Z-QG-TEGMA (b).

The MTG-reactive monomers, Z-QG-EMA and Z-QG-TEGMA, were polymerized with acrylamide as a comonomer to produce Z-QG appended polyacrylamides, P1 and P2, respectively. The composition of each polymer was analyzed by ^1H NMR following removal of unreacted monomers and oligomers by precipitation using acetone. As shown in Table 1,

Table 1. Characteristics of Z-QG Polymers

sample	mole fraction in feed ^d	mole fraction in copolymer ^{a,b}	molecular weight M_w	PDI M_w/M_n	number of Z-QG per polymer chain
P1	0.04/0.96	0.039/0.961	305 000	4.49	31
P2	0.04/0.96	0.036/0.964	334 000	2.98	47

^aMole fraction: Z-QG/acrylamide (mol/mol). ^bMole fraction in copolymer was determined by ^1H NMR.

the mole fractions of Z-QG moieties were ~ 4 mol % for each polymer, which preserved the feed ratio satisfactorily. Gel permeation chromatography analysis revealed that the average molecular weight (M_w) was 305 000 and 334 000 for P1 and P2, respectively, which gave an average number of Z-QG groups per polymer chain of 31 for P1 and 47 for P2.

Conjugation Reaction between Ktag-EGFP and Z-QG Polymers. The Z-QG-modified polyacrylamides (Z-QG polymers) P1 and P2 were reacted with Ktag-EGFP using MTG catalysis and the reaction was analyzed by SDS-PAGE. For each Z-QG polymer, the intensity of the bands around 25 kDa, which corresponds to Ktag-EGFP, decreased and conjugates with high molecular weights were produced in the presence of MTG (Figure 3a). In contrast, wt-EGFP showed no difference, which again indicated the site-specific reaction at the lysine residue in the K-tag of Ktag-EGFP (Supplementary Figure S7). The protein functions of Ktag-EGFP before and after the MTG reaction were examined by fluorescence spectra (Figure 3b). The fluorescence properties of Ktag-EGFP showed minimal change following conjugation to both Z-QG polymers using MTG. This observation indicates that the site-specific

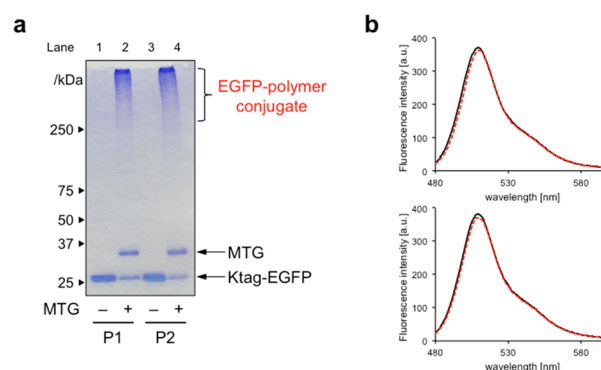


Figure 3. (a) SDS-PAGE analysis of MTG-catalyzed conjugation of Ktag-EGFP with Z-QG polymers. Reaction mixture was incubated at 25 °C for 3 h in 100 mM citrate buffer (pH 5.8). (b) Influence of the MTG reaction on the luminescence of EGFP conjugated with P1 (top) and P2 (bottom). The luminescence spectra were measured before (solid black line) and after (dashed red line) the MTG reaction. $\lambda_{\text{ex}} = 460$ nm, 25 °C.

reaction by MTG enables the production of a protein assembly on a Z-QG polymer without marked loss of protein activities.

The conversion rates of Ktag-EGFP to the conjugates were 57% and 64% for P1 and P2, respectively (Figure 3a, lanes 2 and 4). The slight increase in the reaction rate suggests that the introduction of flexible triethylene glycol linker between the Z-QG and polymer backbone for P2 promotes protein conjugation by the MTG reaction, presumably because of reduced steric hindrance. Therefore, we used the Z-QG polymer P2 for the following study. The influence of the reaction conditions on the conjugation efficiency was further investigated in different buffering solutions. MTG shows a broad optimum pH ranging from 5 to 8 when small molecular weight substrates are used for conjugation.⁴² In the reaction between the Z-QG polymer and Ktag-EGFP, the reaction rate was highly retained between pH 5 to 7 (Supplementary Figure S8a). Interestingly, the conjugation efficiency was greatly influenced by the concentrations of buffer and higher conversions were realized at lower concentrations (Supplementary Figure S8b). The average number of EGFP per polymer chain was calculated to be 1.4, 1.6, and 2.0 at buffer concentrations of 100, 50, 10 mM, respectively. Although the reason for this remains unclear, we assumed that this trend was attributed to the electrostatic interaction between Ktag-EGFP and MTG. The theoretical pI values are 6.2 and 8.9 for Ktag-EGFP and MTG, respectively. Under the present conditions (pH 5–7), MTG is positively charged and Ktag-EGFP is near neutral to slightly negative in charge. The MTG-catalyzed reaction is initiated by the nucleophilic attack on the side chain of the Gln residue by Cys⁶⁴ of MTG, forming a covalently linked Z-QG–MTG intermediate. The intermediate can be further reacted with an acyl-acceptor, Lys of Ktag.⁴² At low concentrations of buffer, we assumed that an electrostatic attraction between the Z-QG–MTG intermediate and Ktag-EGFP facilitates the reaction, while this effect works less efficiently at higher buffer concentrations.

Conjugation Reaction between Ktag-IPP-PG and the Z-QG Polymer. Having the conjugation capacity of Z-QG polymers with K-tagged proteins, we investigated the applicability of the bioconjugation with practical proteins. One desired application of protein assemblies is sensing biomolecules using immunological techniques, such as the

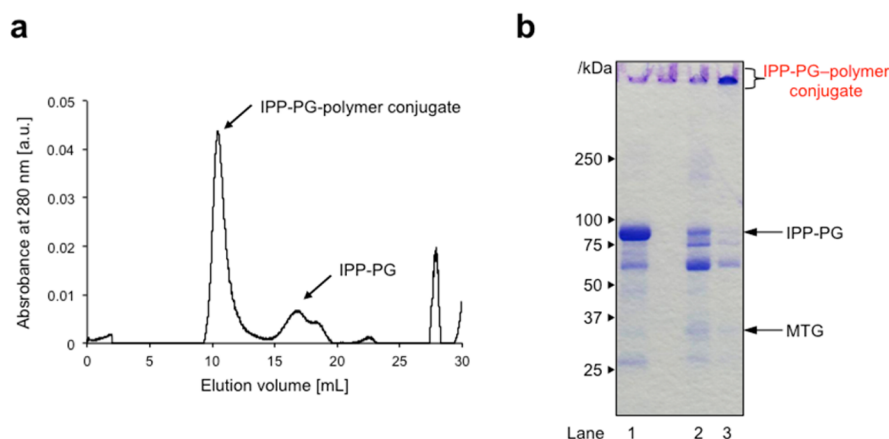


Figure 4. (a) SEC chromatogram of the reaction mixture of IPP-PG–Z-QG polymer 2 (Superdex 200 10/300 GL column). The IPP-PG–Z-QG polymer conjugate was prepared using [Ktag-IPP-PG] = 5 μ M, [Z-QG polymer 2] = 75 μ M in 10 mM acetate buffer (pH 5.6) at 25 $^{\circ}$ C for 6 h. (b) SDS-PAGE analysis of fractions collected by SEC. Lane 1, Ktag-IPP-PG; lane 2, fraction at 17 min; lane 3, fraction at 10 min.

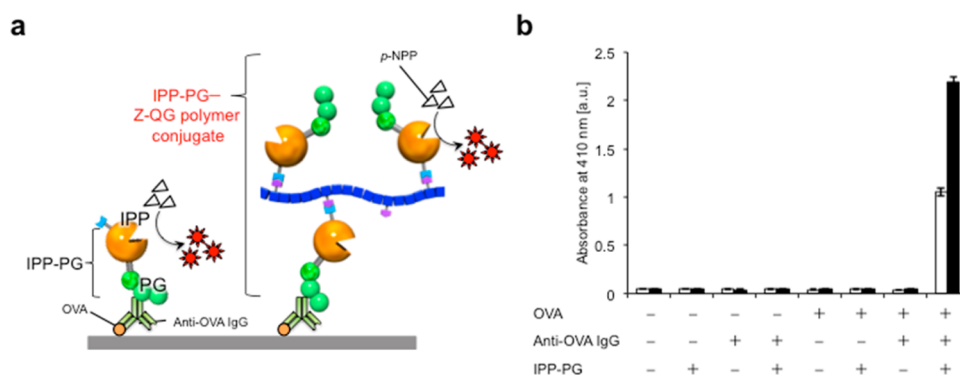


Figure 5. (a) Schematic of detection of ovalbumin (OVA) by enzyme-linked immunosorbent assay (ELISA) using free Ktag-IPP-PG and the IPP-PG–Z-QG polymer conjugate. (b) OVA specific detection of OVA using Ktag-IPP-PG (open) and the IPP-PG–Z-QG polymer conjugate (filled).

enzyme-linked immunosorbent assay (ELISA), Western blotting, and immunochemical staining. In these techniques, enzyme-antibody conjugates, so-called labeled antibodies, are often used to enable the binding to target biomolecules by antibodies and signal production by enzymatic reactions. A chemical conjugation technique is usually applied to produce these labeled antibodies. However, the antibody:enzyme ratio and/or the conjugation sites can vary in each reaction, which may lead to unstable detection of biomolecules.

We previously developed a fusion protein composed of an antibody Fc-binding domain and a chimera alkaline phosphatase, IPP-PG.⁴⁶ The antibody Fc-binding part (PG) was constructed with the C2 and C3 domains of protein G and B domain of protein A. It has been reported that the successive domains of protein G can increase the affinity to antibodies,⁴⁹ and the addition of protein A in between protein G and the enzymatic domain can preserve the activities of each protein.⁵⁰ As an alkaline phosphatase (AP) part, chimera alkaline phosphatase (IPP) composed of intestinal AP and placental AP was employed.⁵¹ The MTG-recognizable K-tag (MRHKGS) was introduced to the C-terminus of IPP-PG (Ktag-IPP-PG). After the confirmation of the produced protein showing the specific detection of biomolecules, the conjugation with the Z-QG polymer was examined. A high reaction ratio was retained at slightly acidic conditions (pH \sim 4.6) when compared with that of the conjugation with Ktag-EGFP (Supplementary Figure S9). We assumed that this was because of the slightly lower theoretical pI value for Ktag-IPP-PG (5.7)

than that for Ktag-EGFP (6.2). The maximum conversion of Ktag-IPP-PG was obtained at pH 5.1, however, unexpected protein degradation and some activity loss of IPP-PG were observed at this pH (Supplementary Figure S10). Therefore, we concluded the optimum buffer for the conjugation of Ktag-IPP-PG on the Z-QG polymer was acetate buffer, pH 5.6. The average number of IPP-PG per polymer chain was calculated to be 2.1 using the average number of Z-QG groups per chain and the reaction rate.

After the MTG reaction, the IPP-PG–Z-QG polymer conjugate was purified by size exclusion chromatography (SEC). The fractions around 10 and 17 min were collected, which were revealed to be the conjugate and free Ktag-IPP-PG, respectively, by SDS-PAGE analysis (Figure 4). The conjugate formation was further analyzed by scanning probe microscopy (SPM). The free Ktag-IPP-PG showed dispersed globular morphologies with approximate heights of 3.5 nm (Supplementary Figure S11a and S12a). In contrast, for the IPP-PG–Z-QG polymer conjugate, string-shaped morphologies were observed (Supplementary Figure S11b). The height profile showed that they barely changed from 3.5 nm, suggesting that these string-shaped structures are composed of one-dimensional clusters of IPP-PG (Supplementary Figure S12b). The observed structures were several tens to a hundred nanometers in length, which may consist of several IPP-PGs.

OVA Detection Using the IPP-PG–Z-QG Polymer Conjugate. The developed IPP-PG–Z-QG polymer conjugate was used for the detection of biomolecules using ELISA. Since

the conjugation site is controlled precisely at the Lys residue in the K-tag, the fusion protein IPP-PG is expected to retain both antibody Fc-binding and enzymatic activity. Ovalbumin (OVA) was used as a model antigen and ELISA was conducted with free Ktag-IPP-PG or the IPP-PG–Z-QG polymer conjugate as a substitution for a secondary antibody in a sandwich assay (Figure 5a). As seen in Figure 5b, the detection signal was observed only when all components existed. This result indicates that specific detection can be achieved using the IPP-PG both in a monomeric state and a conjugate with the Z-QG polymer. Moreover, the detection signal was increased about 2.1-fold with the conjugate compared with that of the free fusion protein. Because the average number of proteins in one polymer chain was determined to be 2.1, the signal amplification was achieved by the clustering of proteins in one structure.

We further tested the sensitivity of the assay using the protein conjugate (Figure 6). Aqueous solutions of OVA at

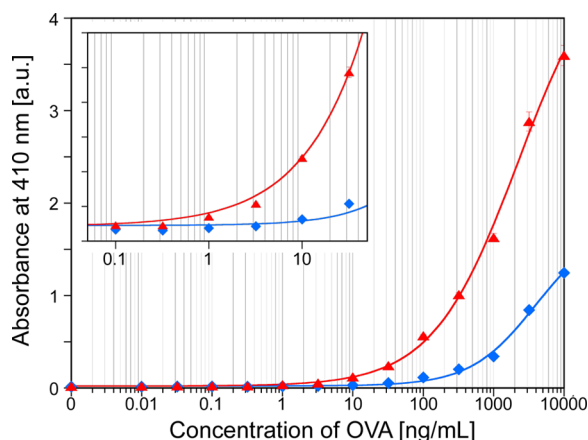


Figure 6. Dose–response detection of OVA using Ktag-IPP-PG (blue, diamonds) and the IPP-PG–Z-QG polymer conjugate (red, triangles).

various concentrations (0–10,000 ng/mL) were incubated in microplates and ELISA was carried out using the procedure mentioned above. The detected signals were plotted against OVA concentrations and the plots were fitted using the following 4-parameter logistic model

$$Y = D + \frac{(A - D)}{\left(1 + \left(\frac{x}{C}\right)^B\right)}$$

where Y is the signal intensity, D is the signal at infinite analyte (OVA in this case) concentration, A is the signal at zero OVA concentration, x is the OVA concentration, C is the inflection point on the curve, and B is the slope factor. The detection limit, defined as 3 sigma of the background signal, was found to be about 1 ng/mL for each system, indicating that the minimum concentration for detection was determined by the affinity of the fusion protein to the antibody. However, the signal amplification using the IPP-PG–Z-QG polymer conjugate was observed over a wide range of OVA concentrations (100–1000 ng/mL) with a maximum of about 5-fold increase when compared with that of free protein.

The signal amplification could be useful for sensing biomolecules in a solid state where a sediment substrate is used for the detection. These include Western blotting and immunohistological staining. We conducted a model system

using dot-blotting; varied concentrations of OVA solutions were blotted on a PVDF membrane and the detection was conducted by the sandwich method. As seen in Figure 7, the

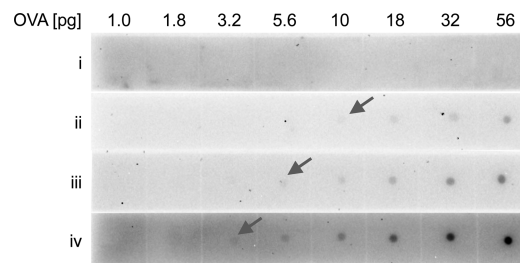


Figure 7. Dot blot detection of OVA using the IPP-PG conjugate. (i) Negative control (without primary antibody); (ii) commercial CIAP-PG; (iii) Ktag-IPP-PG; and (iv) the IPP-PG–Z-QG polymer conjugate. Arrows indicate the detection limit.

fusion protein–Z-QG polymer conjugate could detect OVA at an amount of 3.2 pg on the membrane. On the other hand, when using the unconjugated Ktag-IPP-PG, the lowest amount of OVA that could be detected was 5.6 pg. Although the background was higher with the IPP-PG–Z-QG polymer conjugate, the signal amplification improved the visual detection of biomolecules.

CONCLUSIONS

Research into protein–polymer hybrids has attracted significant attention because of their potential value in industrial applications. Accordingly, protein–polymer fabrication techniques have been developed, although reports on multiple proteins–polymer hybrids are limited and remain challenging to create. This report described the enzymatic preparation of multiple proteins–polymer hybrids using MTG. MTG-recognizable glutamine substrate was introduced to a polyacrylamide and functional proteins appended with a lysine tag were conjugated with the polymer by MTG. The site-specific conjugation retained protein functions on the polymer scaffold. Here, a fusion protein composed of an antibody Fc-binding domain and an enzyme alkaline phosphatase domain was assembled on the polymer and showed immunological detection of specific proteins. The protein clustering effect was clearly shown by an amplification of the detection signals. Although the detection limit was not increased significantly by the conjugate, future studies on the optimization of polymer molecular weights and backbone structures should improve the detection sensitivity. This enzymatic system is a versatile method to fabricate multiple protein assemblies on a synthetic polymer and can be expanded to a wide range of applications, such as cooperative enzyme systems, smart artificial extracellular matrices, and targeted drug delivery carriers.

ASSOCIATED CONTENT

Supporting Information

The Supporting Information is available free of charge on the ACS Publications website at DOI: 10.1021/acs.biomac.6b01538.

Scheme of Z-QG monomers, ^1H and ^{13}C NMR charts of Z-QG monomers and Z-QG polymers, influence of pH, buffer concentration on conjugation reaction between Ktag-EGFP/Ktag-IPP-PG and Z-QG polymers, SPM

analysis of Ktag-IPP-PG–Z-QG polymer conjugate (PDF)

AUTHOR INFORMATION

Corresponding Authors

*(R. W.) E-mail: rie_wakaba@mail.cstm.kyushu-u.ac.jp. Tel: +81 92-802-2809.

*(N.K.) E-mail: nori_kamiya@mail.cstm.kyushu-u.ac.jp. Tel: +81 92-802-2807.

ORCID

Rie Wakabayashi: [0000-0003-0348-8091](https://orcid.org/0000-0003-0348-8091)

Author Contributions

The manuscript was prepared through the contributions of all authors. R.W. and N. K. wrote the manuscript. All authors have given approval to the final version of the manuscript.

Notes

The authors declare no competing financial interest.

ACKNOWLEDGMENTS

The authors are grateful to Ajinomoto Co. Inc. for providing MTG. This work was supported by the Japan Society for the Promotion of Science (JSPS) KAKENHI (B) (No. 25289297, 16H04581) and by the Adaptable and Seamless Technology transfer Program (A-STEP) from the Japan Science and Technology Agency (JST) (AS2321408E).

ABBREVIATIONS

Z-QG, *N*-benzyloxycarbonyl-L-glutaminyglycine; Z-QG-EMA, 2-(*N*-benzyloxycarbonyl-L-glutaminyglycyloxy)-ethyl methacrylate; TEGMA, 2-(2-(2-hydroxyethoxy)ethoxy)ethyl methacrylate; EGFP, enhanced green fluorescent protein; MTG, microbial transglutaminase; SDS-PAGE, sodium dodecyl sulfate polyacrylamide gel electrophoresis; SEC, size exclusion chromatography; ELISA, enzyme-linked immunosorbent assay; OVA, ovalbumin

REFERENCES

- (1) Pasut, G.; Veronese, F. M. *Prog. Polym. Sci.* **2007**, *32*, 933–961.
- (2) Gauthier, M. A.; Klok, H.-A. *Chem. Commun.* **2008**, 2591–2611.
- (3) Fontana, A.; Spolaore, B.; Mero, A.; Veronese, F. M. *Adv. Drug Delivery Rev.* **2008**, *60*, 13–28.
- (4) Le Droumaguet, B.; Nicolas, J. *Polym. Chem.* **2010**, *1*, 563–598.
- (5) Gauthier, M. A.; Klok, H.-A. *Polym. Chem.* **2010**, *1*, 1352–1373.
- (6) Broyer, R. M.; Grover, G. N.; Maynard, H. D. *Chem. Commun.* **2011**, *47*, 2212–2226.
- (7) Hoffman, A. S.; Stayton, P. S. *Prog. Polym. Sci.* **2007**, *32*, 922–932.
- (8) Inada, Y.; Furukawa, M.; Sasaki, H.; Kodera, Y.; Hiroto, M.; Nishimura, H.; Matsushima, A. *Trends Biotechnol.* **1995**, *13*, 86–91.
- (9) Veronese, F. M. *Biomaterials* **2001**, *22*, 405–417.
- (10) Yamamoto, Y.; Tsutsumi, Y.; Yoshioka, Y.; Nishibata, T.; Kobayashi, K.; Okamoto, T.; Mukai, Y.; Shimizu, T.; Nakagawa, S.; Nagata, S.; Mayumi, T. *Nat. Biotechnol.* **2003**, *21*, 546–552.
- (11) Pasut, G.; Veronese, F. M. *J. Controlled Release* **2012**, *161*, 461–472.
- (12) Grotzky, A.; Nauser, T.; Erdogan, H.; Schlüter, A. D.; Walde, P. *J. Am. Chem. Soc.* **2012**, *134*, 11392–11395.
- (13) Grotzky, A.; Altamura, E.; Adamcik, J.; Carrara, P.; Stano, P.; Mavelli, F.; Nauser, T.; Mezzenga, R.; Schlüter, A. D.; Walde, P. *Langmuir* **2013**, *29*, 10831–10840.
- (14) Wilner, O. I.; Weizmann, Y.; Gill, R.; Lioubashevski, O.; Freeman, R.; Willner, I. *Nat. Nanotechnol.* **2009**, *4*, 249–254.
- (15) Teller, C.; Willner, I. *Trends Biotechnol.* **2010**, *28*, 619–628.
- (16) You, C.; Myung, S.; Zhang, Y.-H. P. *Angew. Chem., Int. Ed.* **2012**, *51*, 8787–8790.
- (17) Fu, J.; Yang, Y. R.; Johnson-Buck, A.; Liu, M.; Liu, Y.; Walter, N. G.; Woodbury, N. W.; Yan, H. *Nat. Nanotechnol.* **2014**, *9*, 531–536.
- (18) Kitaoka, M.; Tsuruda, Y.; Tanaka, Y.; Goto, M.; Mitsumori, M.; Hayashi, K.; Hiraishi, Y.; Miyawaki, K.; Noji, S.; Kamiya, N. *Chem. - Eur. J.* **2011**, *17*, 5387–5392.
- (19) Mori, Y.; Nakazawa, H.; Goncalves, G. A. L.; Tanaka, T.; Umetsu, M.; Kamiya, N. *Mol. Syst. Des. Eng.* **2016**, *1*, 66–73.
- (20) Gustafsson, H.; Küchler, A.; Holmberg, K.; Walde, P. *J. Mater. Chem. B* **2015**, *3*, 6174–6184.
- (21) Küchler, A.; Adamcik, J.; Mezzenga, R.; Schlüter, A. D.; Walde, P. *RSC Adv.* **2015**, *5*, 44530–44544.
- (22) Küchler, A.; Bleich, J. N.; Sebastian, B.; Ditttrich, P. S.; Walde, P. *ACS Appl. Mater. Interfaces* **2015**, *7*, 25970–25980.
- (23) Wiedorn, K. H.; Goldmann, T.; Henne, C.; Kühl, H.; Vollmer, E. *J. Histochem. Cytochem.* **2001**, *49*, 1067–1071.
- (24) Yu, X.; Munge, B.; Patel, V.; Jensen, G.; Bhirde, A.; Gong, J. D.; Kim, S. N.; Gillespie, J.; Gutkind, J. S.; Papadimitrakopoulos, F.; Rusling, J. F. *J. Am. Chem. Soc.* **2006**, *128*, 11199–11205.
- (25) Men, D.; Guo, Y.-C.; Zhang, Z.-P.; Wei, H.-P.; Zhou, Y.-F.; Cui, Z.-Q.; Liang, X.-S.; Li, K.; Leng, Y.; You, X.-Y.; Zhang, X.-E. *Nano Lett.* **2009**, *9*, 2246–2250.
- (26) Kitaoka, M.; Mitsumori, M.; Hayashi, K.; Hiraishi, Y.; Yoshinaga, H.; Nakano, K.; Miyawaki, K.; Noji, S.; Goto, M.; Kamiya, N. *Anal. Chem.* **2012**, *84*, 5885–5891.
- (27) Matsunaga, R.; Yanaka, S.; Nagatoishi, S.; Tsumoto, K. *Nat. Commun.* **2013**, *4*, 2211–2220.
- (28) Fierer, J. O.; Veggiani, G.; Howarth, M. *Proc. Natl. Acad. Sci. U. S. A.* **2014**, *111*, E1176–81.
- (29) Hou, L.; Tang, Y.; Xu, M.; Gao, Z.; Tang, D. *Anal. Chem.* **2014**, *86*, 8352–8358.
- (30) Minamihata, K.; Goto, M.; Kamiya, N. *Biotechnol. J.* **2015**, *10*, 222–226.
- (31) Kim, H. K.; Park, T. G. *Enzyme Microb. Technol.* **1999**, *25*, 31–37.
- (32) Rashidian, M.; Dozier, J. K.; Distefano, M. D. *Bioconjugate Chem.* **2013**, *24*, 1277–1294.
- (33) Sato, H.; Hayashi, E.; Yamada, N.; Yatagai, M.; Takahara, Y. *Bioconjugate Chem.* **2001**, *12*, 701–710.
- (34) Fontana, A.; Spolaore, B.; Mero, A.; Veronese, F. M. *Adv. Drug Delivery Rev.* **2008**, *60*, 13–28.
- (35) Mero, A.; Schiavon, M.; Veronese, F. M.; Pasut, G. *J. Controlled Release* **2011**, *154*, 27–34.
- (36) da Silva Freitas, D.; Mero, A.; Pasut, G. *Bioconjugate Chem.* **2013**, *24*, 456–463.
- (37) Popp, M. W.; Dougan, S. K.; Chuang, T.-Y.; Spooner, E.; Ploegh, H. L. *Proc. Natl. Acad. Sci. U. S. A.* **2011**, *108*, 3169–3174.
- (38) Qi, Y.; Amiram, M.; Gao, W.; McCafferty, D. G.; Chilkoti, A. *Macromol. Rapid Commun.* **2013**, *34*, 1256–1260.
- (39) DeFrees, S.; Wang, Z.-G.; Xing, R.; Scott, A. E.; Wang, J.; Zopf, D.; Gouty, D. L.; Sjöberg, E. R.; Panneerselvam, K.; Brinkman-Van der Linden, E. C. M.; Bayer, R. J.; Tarp, M. A.; Clausen, H. *Glycobiology* **2006**, *16*, 833–843.
- (40) Rashidian, M.; Song, J. M.; Pricer, R. E.; Distefano, M. D. *J. Am. Chem. Soc.* **2012**, *134*, 8455–8467.
- (41) Carrico, I. S.; Carlson, B. L.; Bertozzi, C. R. *Nat. Chem. Biol.* **2007**, *3*, 321–322.
- (42) Ando, H.; Adachi, M.; Umeda, K.; Matsuura, A.; Nonaka, M.; Uchio, R.; Tanaka, H.; Motoki, M. *Agric. Biol. Chem.* **1989**, *53*, 2613–2617.
- (43) Strop, P. *Bioconjugate Chem.* **2014**, *25*, 855–862.
- (44) Mori, Y.; Wakabayashi, R.; Goto, M.; Kamiya, N. *Org. Biomol. Chem.* **2013**, *11*, 914–922.
- (45) Abe, H.; Goto, M.; Kamiya, N. *Chem. - Eur. J.* **2011**, *17*, 14004–14008.
- (46) Hayashi, K.; Tomozoe, Y.; Nagai, K.; Matsuba, K.; Mitsumori, M.; Hiraishi, Y.; Matsumura, T.; Ueda, H.; Kamiya, N. *Kagaku Kogaku Ronbunshu* **2015**, *41*, 38–42.

- (47) Schneider, C. A.; Rasband, W. S.; Eliceiri, K. W. *Nat. Methods* **2012**, *9*, 671–675.
- (48) Kashiwagi, T.; Yokoyama, K.-i.; Ishikawa, K.; Ono, K.; Ejima, D.; Matsui, H.; Suzuki, E. — i. *J. Biol. Chem.* **2002**, *277*, 44252–44260.
- (49) Sato, S.; Religa, T. L.; Daggett, V.; Fersht, A. R. *Proc. Natl. Acad. Sci. U. S. A.* **2004**, *101*, 6952–6956.
- (50) Maeda, Y.; Ueda, H.; Kazami, J.; Kawano, G.; Suzuki, E.; Nagamune, T. *Anal. Biochem.* **1997**, *249*, 147–152.
- (51) Sasajima, Y.; Kohama, Y.; Kojima-Misaizu, M.; Kurokawa, N.; Hara, Y.; Dong, J.; Ihara, M.; Ueda, H. *Mol. Biotechnol.* **2014**, *56*, 953–961.